Pulsed Magnetron Sputtering: The Role of the Applied Power on W Coatings Properties

Ioana-Laura Velicu[1(✉)], Vasile Tiron[2], Ilarion Mihaila[3], and Claudiu Costin[1]

[1] Iasi Plasma Advanced Research Center (IPARC), Faculty of Physics, Alexandru Ioan Cuza University of Iasi, 700506 Iasi, Romania
laura.velicu@uaic.ro
[2] Research Department, Faculty of Physics, Alexandru Ioan Cuza University of Iasi, 700506 Iasi, Romania
[3] Integrated Center of Environmental Science Studies in the North-Eastern Development Region (CERNESIM), Alexandru Ioan Cuza University of Iasi, 700506 Iasi, Romania

Abstract. The interaction of low/high density transient plasma with tungsten (W) target was investigated *via* the sputtered material: in the gas phase, measuring the ion energy distribution function, and as deposited coatings, analyzing the compositional, structural, morphological, mechanical and tribological properties. The W target was sputtered in Ar atmosphere, at two different target power densities (instantaneous peak values of 0.2 and 3 kW/cm^2), using a pulsed magnetron discharge. All obtained coatings were polycrystalline. A porous columnar structure was observed for the films deposited at low target power density, while denser-than-bulk films were obtained at high target power density. Comparing the high and low power modes, the W^+ ion flux is seven times higher in the first case, while the deposition rate is three times higher in the second one.

Keywords: Tungsten coatings · Pulsed magnetron sputtering · Mass spectrometry · Tribological properties

1 Introduction

Magnetron sputtering is a well-known deposition technique designed to produce coatings, from a large variety of materials, both for basic research and industrial purpose. In the last two decades, the magnetron sputtering was extensively operated in high power pulsed mode, being generally known in the literature as High Power Impulse Magnetron Sputtering (HiPIMS) [1]. In HiPIMS, a high power density (several kW/cm^2) applied to the magnetron target in unipolar pulses, at low duty cycle and low repetition frequency, facilitates the generation of high density plasma, with high ionization degree (>70%) [2] and broad energy distribution function of the sputtered species [3]. The high ion-to-neutral ratio and intense energetic particle bombardment have been shown to enable the deposition of ultra-dense and smooth metallic and

D. Luca et al. (eds.), *Recent Advances in Technology Research and Education*, Advances in Intelligent Systems and Computing 660, DOI 10.1007/978-3-319-67459-9_24

compound films, allowing to tailor the phase composition, microstructure and morphology, the elemental composition and, subsequently, the properties and functionality of deposited coatings [4].

Beside the well-known application in thin films deposition, the magnetron discharge, operated in high power pulse mode, is suitable to simulate critical aspects of the plasma-wall interaction under fusion devices relevant conditions, the power density applied on the magnetron cathode [5, 6] being comparable with the one expected to be delivered to the ITER divertor (10 MW/m^2) [7]. In such experiments, the selection of the plasma facing material is of great importance. Due to its low erosion yield and high melting temperature, tungsten (W) is one of the most promising plasma-facing material for fusion devices, used in both bulk and thin film (deposited on carbon tiles) form. Hence, the present work reports on the use of the magnetron discharge for fusion related experiments, both as deposition device and as plasma-wall interaction model system. Regarding the deposition device, we studied the role of the applied power on the properties of the deposited W coatings. Such coatings are proposed to cover the carbon fiber composite (CFC) tiles of the wall and/or divertor of future tokamaks [7]. As plasma-wall interaction model, we studied W erosion under low/high density plasma bombardment, by measuring the ionized sputtered material flux. Details of the experiment, analysis techniques and results follow in the next sections.

2 Experimental Set-up

The W coatings were deposited in a high vacuum deposition system using the pulsed magnetron sputtering technique. The magnetron was housed in a vacuum chamber (40 cm in length and 40 cm in diameter) which was pumped to a base pressure of 10^{-5} Pa, using a turbomolecular pump backed by a dry scroll pump. The W planar target (99.995% purity, disk-shape, 5 cm in diameter and 3 mm thickness) was sputtered in pure argon atmosphere, at 1 Pa pressure, by applying low (500 V) and high (1000 V) discharge voltage, in pulses of 10 μs. The short-pulse regime was obtained using a fast pre-ionized high-power pulsed-magnetron sputtering system [8]. For each mode, the pulsing frequency was varied in order to maintain a constant average power of 100 W, which corresponds to a frequency of 3 kHz for low voltage and 500 Hz for high voltage, respectively. Tungsten coatings were deposited on grounded and unintentionally heated molybdenum (Mo) substrates, by setting the deposition time to 100 min. The substrate (disk-shape, surface area of 5 cm^2) was placed at 10 cm in front of the target, axially aligned to it. During the deposition process, time-averaged ion energy distribution functions (IEDFs) of both gas and sputtered material were recorded with an energy resolving mass spectrometer (EQP 1000 Hiden Analytical), facing directly the target surface from the substrate position. Simultaneously, the deposition rate was monitored by a quartz crystal microbalance mounted in the vicinity of the substrate. The analysis of the deposited coatings was made by Atomic Force Microscopy (AFM) and Scanning Electron Microscopy (SEM) for topological and morphological characterization and by X-Ray Diffraction (XRD) and Rutherford Backscattering Spectrometry (RBS) for structural characterization. For mechanical and tribological properties, nanoindentation and nanoscratch tests were performed using a

Nanoindentation Tester (NHT2) equipped with a three-sided diamond pyramidal Berkovich indenter tip with an average radius of curvature of about 100 nm and a Micro-Scratch Tester (MST) equipped with a Rockwell type indenter (100 Cr6, 100 μm radius), both from CSM Instruments. The nanoindentation data were analyzed with the Oliver-Pharr method.

3 Results and Discussion

The temporal evolution of the instantaneous discharge power delivered to the magnetron target, during one pulse at low and high target voltage, is illustrated in Fig. 1a. A peak current of about 4 A was reached during the low voltage pulse, while 36 A was the maximum current value for the high voltage pulse, the corresponding peak power density on the target surface being 0.2 and 3 kW/cm^2, respectively. The two working regimes will be further referred as low and, respectively, high power mode, even if the average power is the same for both of them. In order to investigate the influence of the applied power on the metal ion flux towards the substrate, the energy distribution function of the sputtered material (W) resulted in ionized state was measured with the energy resolved mass spectrometer. The twofold purpose of this diagnostic was: the correlation of the metal ion flux with the deposited coatings properties (surface morphology, microstructure, density, adhesion, hardness, Young's modulus, and coefficient of friction) and the knowledge of W^+ ion energy distribution function, when W^+ ion is seen as impurity in the discharge. The W^+ IEDF (Fig. 1b) recorded for the high power mode (HiPIMS) is much broader, with a significantly more energetic tail, and contains a larger fraction of both low and high energy ions as compared to that recorded in the low power mode. The W^+ ion flux (proportional to the integral of the IEDF) obtained in HiPIMS mode is seven times higher as compared to the ion flux recorded in low discharge power mode.

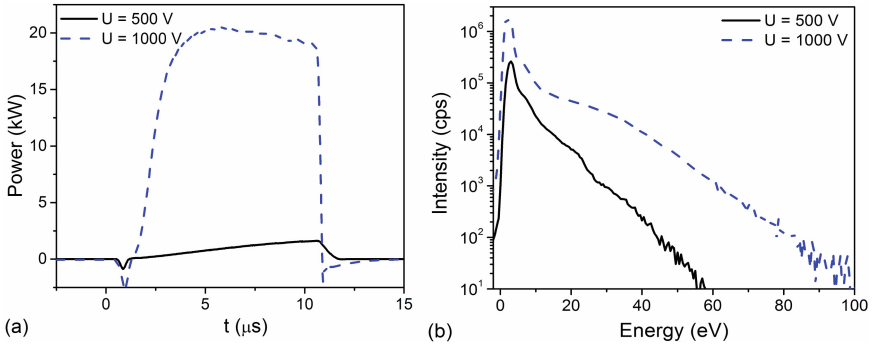

Fig. 1. (a) Temporal evolution of the discharge power and (b) time-averaged ion energy distribution function of W^+, in low and high power pulsed magnetron sputtering.

The low metal ion flux at the substrate, registered in low power mode, shows that this operation mode behaves more like direct current magnetron sputtering (DCMS) than HiPIMS mode. This aspect is well illustrated in Fig. 2 which shows the W deposition rate as a function of discharge voltage.

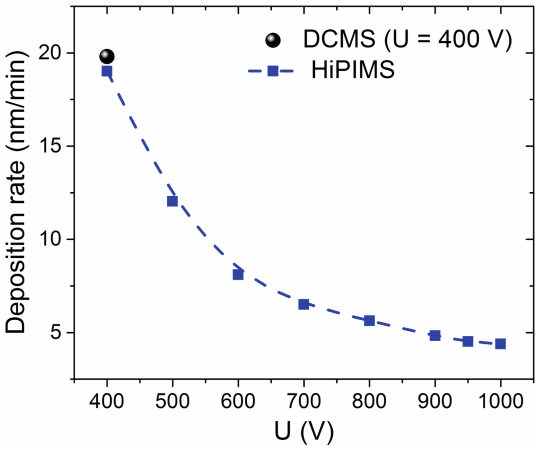

Fig. 2. Deposition rate as a function of the discharge voltage, measured at the same average power of 100 W.

By reducing the discharge voltage from 1000 V to 400 V, the deposition rate gradually increases from 4.5 to 19 nm/min, its maximum value being very close to that obtained in DCMS regime, for the same average power. The main cause for the loss in deposition rate in HiPIMS is the fact that the ionization degree of the sputtered atoms is very high and a large fraction of metallic ions is back-attracted to the target, resulting also in a self-sputtering process. In addition, the metal ion fraction returning to the target contributes to the peak current, a very important parameter included in the power normalized deposition rate. Therefore, the loss deposition rate in HiPIMS is strongly related to the target peak current.

We demonstrated in a previous work [9] that the power normalized deposition rate decreases as the peak current increases. The peak target current was controlled by certain magnetron operation parameters such as: target voltage, pulse duration, magnetic field, target erosion depth, and HiPIMS operation mode. Recently, Greczynski *et al.* have found that the power normalized deposition rates in HIPIMS decays exponentially with the peak target current increasing [10]. In our experiments, the peak current showed a linear increase with the increase of the target voltage (not shown here).

Despite a lower deposition rate as compared to DCMS, HiPIMS technique still represents a powerful deposition technique due to its high metal ion flux directed towards the growing film. It is expected that the intense and energetic metal ion bombardment during magnetron sputtering, in high power mode, to improve the properties of the coatings due to a higher surface activation energy delivered at the growing film surface and increased adatoms mobility. The influence of the applied power (and thus metal ion flux) on the coatings properties (crystallinity, microstructure, packing density, adhesion, hardness, Young's modulus, coefficient of friction) is discussed below.

The crystallinity and crystal orientation of W deposited coatings were investigated by X-ray diffraction. The diffraction patterns (Fig. 3) indicate, in both cases, polycrystalline structure with a preferential growth of W (200) phase ($2\theta \approx 58°$). HiPIMS mode leads to

a higher crystalline structure, revealed by the higher intensity of the diffraction peaks. The crystallite size was estimated from dominant W (200) peak, using the Debye–Scherrer formula. The HiPIMS deposition technique tends to produce films with larger nanocrystallites as compared to the low power pulsed deposition technique. The size of nanocrystallites increased when the applied power was also increased, from 40 to 54 nm.

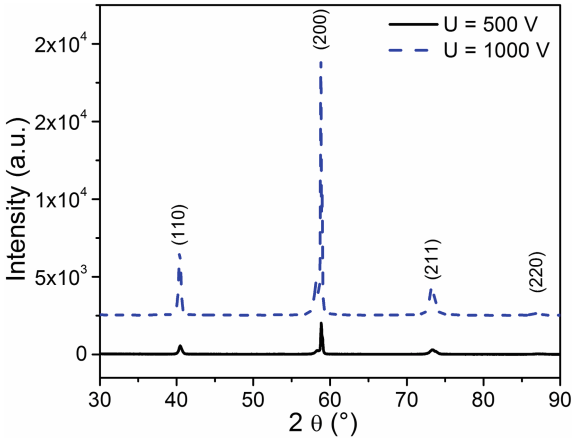

Fig. 3. XRD patterns of W coatings deposited by low/high power pulsed magnetron sputtering.

SEM and AFM images of W deposited coatings are shown in Fig. 4. The cross-sectional SEM image of the coating deposited at low power reveals a porous columnar structure, while the coating deposited at high power shows a very dense structure and smooth surface. Although the deposition time and the average power were the same in both cases, the thickness of the W coating deposited in HiPIMS regime (≈400 nm) is three times lower as compared to that of the coating deposited in low power magnetron sputtering regime (≈1270 nm). This difference has two main reasons: (i) the higher coating density and (ii) the lower deposition rate in HiPIMS mode as compared to low power pulsed magnetron sputtering. The density of the deposited W coatings was estimated by measuring the areal atomic density using Rutherford backscattering spectrometry and the coating thickness from cross-sectional SEM images [11]. The measurements showed that the mass-density of W coatings deposited in low power magnetron sputtering regime is approximately 8% lower than the mass-density of the bulk W (19.25 g/cm^3), while the W coatings deposited by HiPIMS is about 5% denser than the reported bulk value. The enhanced mass-density of W coatings deposited by HiPIMS may be attributed to the intense and energetic bombardment of the growing film, as well as to the increased fraction of ionized metal flux [12]. Compared to low power pulsed magnetron sputtering, in HiPIMS the sputtered metal flux is highly ionized and it is subjected to strong back-attraction effect caused by the high negative voltage applied to the target. Self-sputtering, gas rarefaction, a less than linear increase in sputtering yields with target voltage and side-wall

loss of metal ions, all these processes represent other important factors decreasing the deposition rate in HiPIMS [13]. The back-attraction effect is strongly reduced when operating with very short pulses [14].

In order to analyze and compare the surface roughness of the deposited coatings, three random areas of 3×3 μm^2 were scanned over the surface for each deposited sample. The root mean square (RMS) roughness values were calculated using image processing software. For the W coatings deposited by low power pulse magnetron sputtering, the mean value of the RMS roughness is about 14.4 nm, while the RMS roughness of the coating deposited in HiPIMS mode is 1.2 nm (very smooth surface, with very fine grain sizes). The lower roughness obtained using HiPIMS may be attributed to the high mobility of the adatoms induced by the growing film bombardment with highly energetic ions (see Fig. 1b). Increasing the target voltage, the RMS roughness of the surface decreases and the grains have smaller sizes, being more homogenously distributed on the coating's surface. Therefore, during film growth process in HiPIMS regime, the intense ion bombardment improves the surface mobility, leading to enhanced packing density and smoother surface by removing asperities, voids and defects in the material.

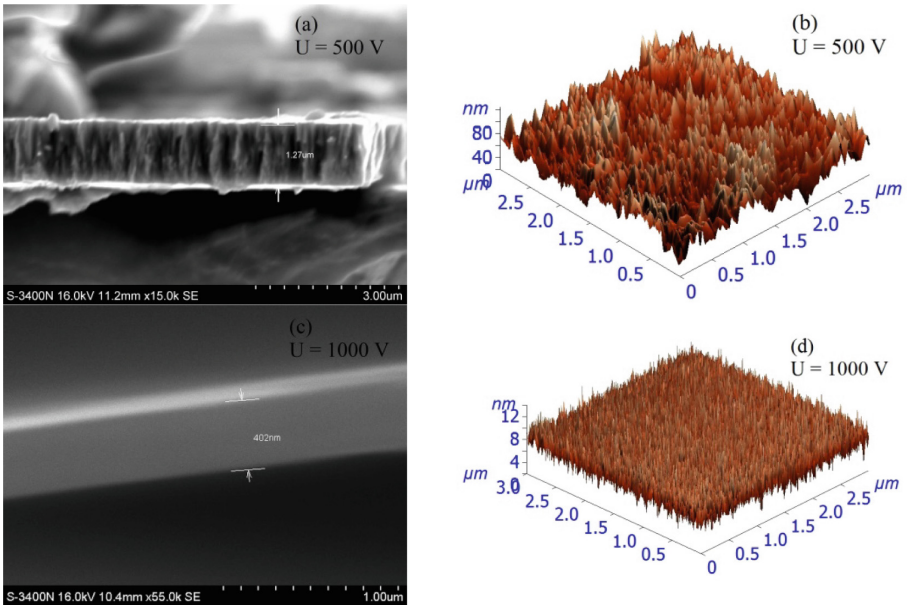

Fig. 4. Cross-sectional SEM (a, c) and 3D AFM (b, d) images for W coatings deposited by low (a, b) and high (c, d) power pulsed magnetron sputtering.

Load-controlled indentation tests were performed at room temperature, on each sample, to determine hardness and absolute Young's modulus values. In order to minimize the Mo substrate influence on the indentation data, the indentation depth was

limited to less than 15% of the coating thickness. It was found that the coatings deposited in high discharge power mode have higher hardness and Young's modulus values as compared to those of the coatings deposited in low power mode. Hardness and absolute Young's modulus values are listed in Table 1. The improvements in hardness may be correlated with the observed densification of the coatings deposited in HiPIMS mode. Coatings with columnar structures contain voids which allow deformation and movement of dislocations in the material when a load is applied [15]. Due to reduced voids, coatings with denser structure exhibit a good resistance to deformation and limit the propagation of dislocations.

In order to study the critical loads (Lc_1 – cohesive failure, Lc_2 – adhesive failure) of the W coatings, linear and progressive-load scratches were performed on each sample, on different surface location, by linearly increasing the load applied on the indenter from 0 to 20 N (0.5 N/min loading rate). Lc_1 and Lc_2 values increase from approximately 5 N and 10 N for coatings deposited by low power pulsed magnetron to 15 N and 17 N, respectively, for the W coatings deposited by HiPIMS.

The coefficient of friction was measured as friction force divided by the applied normal load. The coefficient of friction is generally known to decrease with an increase in hardness and decrease in the roughness [16]. In our case, the coatings deposited in HIPIMS mode show significant improvement in friction resistance (see Table 1) as compared to W coatings deposited in low power pulse mode due to higher hardness and much lower RMS roughness value.

Table 1. Values of deposition rate (S), RMS surface roughness (R_{RMS}), hardness (H), absolute Young's modulus (E), coefficient of friction (μ) and critical loads (Lc_1 and Lc_1) for W coatings deposited by low (500 V) and high (1000 V) power pulsed magnetron sputtering.

U (V)	S (nm/min)	R_{RMS} (nm)	H (GPa)	E (GPa)	μ	Lc_1 (N)	Lc_2 (N)
500	19.2	14.4	20.5	348	0.05	5	10
1000	4.2	1.2	25.2	392	0.03	15	17

4 Conclusion

The sputtering process of a W target by high and low power pulsed magnetron discharge was analyzed from two perspectives: the deposited coatings and the energy distribution function of the ionized sputtered material. The deposited films were characterized, in term of morphology and structure, by Atomic Force Microscopy, Scanning Electron Microscopy, X-Ray Diffraction and Rutherford Backscattering Spectrometry. W sputtered material was investigated in the gas phase by Mass Spectrometry. The deposited coatings have polycrystalline structure, with a preferential growth of W (200) phase, having a higher crystalline structure when is deposited in HiPIMS mode. The coatings deposited at low instantaneous power reveal a porous columnar structure, with a RMS surface roughness of about 14.4 nm and lower mass-density than bulk, while the coatings deposited at high instantaneous power show a very dense structure, with a RMS surface roughness of about 1.2 nm and higher mass

density than the bulk. The W^+ ion flux, measured at the substrate position, in high power mode, is seven times higher than the ion flux recorded in low power mode, while the deposition rate is three times lower. The observed changes in texture, surface morphology and coatings density with the applied power are a result of the increased ion flux and increased mobility on the surface which caused an evolution from rough surface and columnar structure to a very smooth surface and fully dense structure, with high hardness and elastic modulus, good adhesion to the substrate and low coefficient of friction.

Acknowledgment. This work has been carried out within the framework of the EUROfusion Consortium and has received funding from the Euratom research and training programme 2014–2018 under grant agreement No 633053. The views and opinions expressed herein do not necessarily reflect those of the European Commission. The project has also received funding from the Romanian National Education Minister/Institute of Atomic Physics under contract 1EU-1/2/2016.

References

1. Gudmundsson, J.T., Brenning, N., Lundin, D., Helmersson, U.: J. Vac. Sci. Technol., A **30**, 030801 (2012)
2. Helmersson, U., Lattemann, M., Bohlmark, J., Ehiasarian, A.P., Gudmundsson, J.T.: Thin Solid Films **513**, 1–24 (2006)
3. Greczynski, G., Hultman, L.: Vacuum **84**, 1159–1170 (2010)
4. Samuelsson, M., Lundin, D., Jensen, J., Raadu, M.A., Gudmundsson, J.T., Helmersson, U.: Surf. Coat. Technol. **205**, 591–596 (2010)
5. Tiron, V., Velicu, I.-L., Porosnicu, C., Burducea, I., Dinca, P., Malinský, P.: Appl. Surf. Sci. **416**, 878–884 (2017)
6. Dinca, P., Porosnicu, C., Butoi, B., Jepu, I., Tiron, V., Pompilian, O.G., Burducea, I., Lungu, C.P., Velicu, I.-L.: Surf. Coat. Technol. **321**, 397–402 (2017)
7. Federici, G., et al.: Nucl. Fusion **41**, 1967–2137 (2001)
8. Konstantinidis, S., Dauchot, J.P., Ganciu, M., Ricard, A., Hecq, M.: J. Appl. Phys. **99**, 013307 (2006)
9. Tiron, V., Velicu, I.-L., Vasilovici, O., Popa, G.: J. Phys. D Appl. Phys. **48**, 495204 (2015)
10. Greczynski, G., Hultman, L.: Vacuum **124**, 1–4 (2016)
11. Velicu, I.-L., Tiron, V., Rusu, B.G., Popa, G.: Surf. Coat. Technol. (2016) doi:10.1016/j.surfcoat.2016.11.001
12. Velicu, I.-L., Tiron, V., Porosnicu, C., Burducea, I., Lupu, N., Stoian, G., Popa, G., Munteanu, D.: Appl. Surf. Sci. (2017) doi:10.1016/j.apsusc.2017.01.067
13. Anders, A.: J. Vac. Sci. Technol., A **28**, 783 (2010)
14. Antonin, O., Tiron, V., Costin, C., Popa, G., Minea, T.M.: J. Phys. D Appl. Phys. **48**, 015202 (2015)
15. Ehiasarian, A.P., Vetushka, A., Aranda Gonzalvo, Y., Sáfrán, G., Székely, L., Barna, P.B.: J. Appl. Phys. **109**, 104314 (2011)
16. Bhushan, B.: Introduction to tribology, 2nd edn. Wiley, NewYork (2013)